H-D Support Set: Identifying Frequency Dynamics by Constraining Multidimensional Frequency Parameter Bounds

Yiping Yuan, Member, *IEEE*, Liqian Zhu, Student Member, *IEEE*, Zhenyuan Zhang, Senior Member, *IEEE*, Weihao Hu, Senior Member, *IEEE*, Zhe Chen, Fellow, *IEEE*

***Abstract*—Existing research on the system frequency response (SFR) and frequency-oriented studies primarily relies on the commonly-used metrics such as rate-of-frequency-change (RoCoF), nadir, and quasi-steady-state (Qss). Nevertheless, the complex interdependencies among these multidimensional frequency parameters have not been fully explored. This letter introduces a new criterion, termed as H-D support set, to assess frequency stability by considering multidimensional relationships between these frequency parameters. An analytical solution is derived to quantify these interdependencies, and a convex polygon representation is constructed to visualize the feasible operating region defined by these parameters. Using this criterion, the impact of different frequency parameter configurations on system stability can be clearly obtained and analyzed. The effectiveness of the proposed approach is demonstrated on a modified IEEE 30-bus test system.**

***Index Terms*—System frequency response, H-D support set, multidimensional frequency parameters.**

I. Introduction

THE low inertia character of electrical power system significantly impact the system frequency security, which implicitly change the scheduling commitment results provided by different generators. In such circumstances, existing studies about power system dynamic response [1], [2], storage device sizing and control parameter tunning [3], optimal scheduling operation [4]–[6], and even medium-term & long-term generation planning studies [7], [8], trends to emphasis the consideration of frequency response and frequency stability.

The primary objective of frequency-oriented studies as previously discussed is to ascertain the security of frequency dynamic, while it can be described through the SFR function, typically expressed by multidimensional frequency parameters, including system-level/regional-level $inertia$, $damping$, $droop$, and $reserve$, etc. Conventional methodologies establish dynamic frequency criteria, typically expressed as mathematical constraints such as RoCoF, nadir and Qss [1]–[8]. These criteria define a feasible operating region within which frequency dynamics are deemed secure. System stability is subsequently evaluated by determining if the observed frequency derivation derived from the SFR function remains within this defined region.

Nevertheless, these conventional approaches suffers from an implicitly limitation: it provides only a qualitative assessment of the current frequency parameter configuration's reasonableness. While it can determine if the system operates within predefined (frequency dynamic) limits, it fails to explicitly delineate the precise safety boundaries of these multidimensional frequency parameters. Consequently, it can neither directly quantify the margins of safety, nor provide actionable insights into how to adjust these parameters to enhance system frequency security.

This letter introduces a new criterion, termed as H-D Support Set, to access the feasible bounds of multidimensional frequency parameters. Furthermore, an open-source tool (repository address: https://github.com/Divas1234/frequencyregions.git) for H-D Support Set simulation is made freely available. Leveraging the SFR theorem, the interaction between these parameters is analyzed, and both the upper and lower bounds of the frequency parameter bounds are explicitly calculated. In contrast to existing methodologies, the proposed approach provides a well-defined boundary interval for frequency parameters, thereby enabling more effective tuning optimization of frequency control parameters and facilitating comprehensive frequency dynamic analysis.

II. SFR theorem in low inertia power systems

Given such a low inertia power systems that considers high penetration of converters, the uniform analytical expression of frequency dynamic processes can be written as,

$$\Delta f(s)=\frac{1+sT}{2H_{EQU}T_G(s^2+2\zeta\omega_n s+\omega_n^2)}\frac{\Delta P_{Step}}{s} \tag{1a}$$

$$\omega_n=\sqrt{\frac{D_{EQU}+R_G}{2H_{EQU}T_G}},\zeta=\frac{2H_{EQU}+T_G(D_{EQU}+F_G)}{2\sqrt{2H_{EQU}T_G(D_{EQU}+R_G)}} \tag{1b}$$

where $\Delta f(s)$ represents the frequency derivation with a step-type power disturbance ΔP_{Step}, H_{EQU},D_{DEQ}, respectively, describes the equivalent inertia parameter and damping parameter. T_G is the time constant of conventional generator, R_G denotes the aggregated droop parameter generated by conventional generators, F_G denote the fraction of total power generated by high pressure turbines of conventional generators. In these formulations, the time constants within the transfer function of $\Delta f(s)$ are normalized to unity, and the response times of converters with diverse control schemes are approximated as negligible. A more detailed feasibility analysis is provided in [3].

In correlation with (1), the maximum frequency deviation termed as $\max[\Delta f(t)]$ as well as the maximization rate of frequency change termed as $\max[\Delta f'(t)]$ can be derived as below,

$$\max[\Delta f(t)] = \Delta f(t)|_{t=t^k_{nadir}} = -\frac{\Delta P_{Step}}{D_{EQU}+R_G}\Bigg(1+ (-1)^k\sqrt{\frac{T_G(R_G-F_G)}{2H_{EQU}}}e^{-\zeta\omega_n t^k_{nadir}}\Bigg) \tag{2a}$$

$$t^k_{nadir} = \frac{1}{\omega_d}\arctan\left(\frac{\omega_d}{\zeta\omega_n - T_G^{-1}}\right)+\frac{k\pi}{\omega_d}$$

$$\omega_d=\omega_n\sqrt{1-\zeta^2},\quad \phi=\sin^{-1}\left(\sqrt{1-\zeta^2}\right)$$

$$\max[\Delta f'(t)] = \Delta f'(t)|_{t=t_0} = \frac{1}{2}H^{-1}_{EQU}\Delta P_{Step} \tag{2b}$$

$$\Delta f_{QSS}(t) = \Delta f(t)|_{t=t_\infty} = D^{-1}_{EQU}\Delta P_{Step} \tag{2c}$$

where $\max[\Delta f(t)]^k$ enforces the maximum frequency deviation at the k-th cycle, $\max[\Delta f'(t)]$ defines the maximum

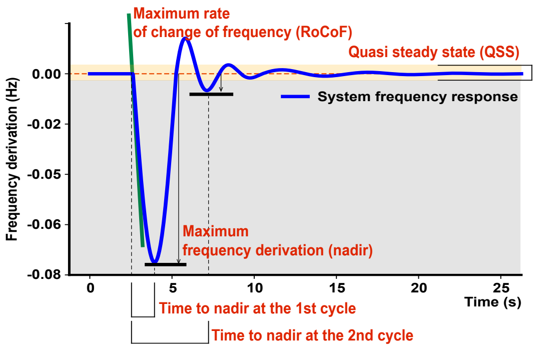

Fig. 1. The frequency dynamic process in the low inertia power system

rate of change of frequency derivation, $\Delta f_{QSS}(t)$ denotes the (quasi) steady-state frequency deviation, t^k_{nadir} denotes the time to the k-th nadir of the frequency deviation.

To ensure the security of frequency dynamics across the entire frequency response processes, the amounts of $\max[\Delta f(t)]$, $\max[\Delta f'(t)]$ and $\Delta f_{QSS}(t)$ must be constrained within the predefined frequency dynamic restrictions, as discussed in existing frequency-oriented studies,

$$\begin{cases} Nadir\ constraint: & \max[\Delta f(t)] \leq \gamma_{Nadir} \\ RoCoF\ constraint: & \max[\Delta f'(t)] \leq \gamma_{RoCoF} \\ QSS\ constraint: & \Delta f_{QSS}(t) \leq \gamma_{QSS} \end{cases} \tag{3a}$$

where γ_{Nadir}, γ_{RoCoF} and γ_{QSS} are predefined frequency dynamic restrictions concerning frequency nadir, RoCoF, and QSS frequency derivation, respectively.

III. H-D Support Set: A New Criterion for Frequency Security Identification

This section derives explicit bounds of multidimensional frequency parameters, including inertia, damping, and droop gains, these bindings result in a new criterion for frequency security identification that differs from (3a).

The sufficient condition for the occurrence of maximum frequency derivation (nadir) is predicated on the convergence of the transfer function (1a) and the non-negativity characteristic of time-to-nadir coefficient. For the first category, this translates to the mathematical requirement that all poles, as derived from the denominator of (1a), must lie within the left half of the complex s-plane. Since the amount of poles in (1a) can be written as $-\zeta\omega_n \pm \omega_n\sqrt{1-\zeta^2}$, $\zeta \geq 0$ must hold to ensure the convergence of the transfer function. For the latter category, the amount of denominator should be positive to guarantee the non-negativity of time-to-nadir coefficient, that is, $\zeta\omega_n - T_G^{-1} \geq 0$, and $\sqrt{1-\zeta^2} \geq 0$. So, the determination conditions for the intermediate variables, ζ, ω_n, can be obtained,

$$0 \leq \zeta \leq 1, \quad \zeta\omega_n \geq \frac{1}{T_G} \tag{4a}$$

Substituting (1b) into (4a), the bounds of inertia and damping parameters can be derived as below,

$$H_{EQU} \leq \frac{1}{2}T_G\left(\text{term}_1 + \sqrt{\text{term}_2}\right) \tag{5a}$$

$$H_{EQU} \geq \frac{1}{2}T_G\left(\text{term}_1 - \sqrt{\text{term}_2}\right) \tag{5b}$$

$$H_{EQU} \leq \frac{1}{2}(D_{EQU} + F_G)T_G \tag{5c}$$

$$\text{term}_1 = (D_{EQU} - F_G + 2R_G) \tag{5d}$$

$$\text{term}_2 = (D_{EQU} - F_G + 2R_G)^2 - (D_{EQU} + F_G)^2 \tag{5e}$$

$$\text{term}_2 \geq 0 \Longrightarrow (R_G - F_G)(R_G + D_{EQU}) \geq 0 \tag{5f}$$

Let $H_{EQU} = \mathcal{Q}(D_{EQU})$, the relationship between H_{EQU} and D_{EQU} can be derived as below,

$$\overbrace{\tfrac{1}{2}T_G\left(\text{term}_1 - \sqrt{\text{term}_2}\right)}^{lower\ bound} \leq H_{EQU} = \mathcal{Q}(D_{EQU}) \leq \underbrace{\min\left[\ \tfrac{1}{2}T_G\left(\text{term}_1 + \sqrt{\text{term}_2}\right), \tfrac{1}{2}(D_{EQU} + F_G)T_G\ \right]}_{upper\ bound} \tag{6a}$$

Next, other relations between H_{EQU} and D_{EQU} concerning nadir, RoCoF, and Qss, can be extended from (3a). For simplification, let $\max[\Delta f(t)] = \mathcal{R}(H_{EQU}, D_{EQU})$ denotes the non-linear close form of (2a), then, more bindings between H_{EQU} and D_{EQU} can be derived as below,

$$H_{EQU} \geq \underbrace{\max\left[\tfrac{1}{2}\gamma^{-1}_{RoCoF}\Delta P_{Step}, \mathcal{R}^{-1}(D_{EQU})\gamma_{Nadir}\right]}_{lower\ bound} \tag{7a}$$

$$D_{EQU} \geq \gamma^{-1}_{QSS}\Delta P_{Step} \tag{7b}$$

By further meticulously organizing the preceding derivations, a concise bounds for system inertia and damping parameters can be estimated from (6) and (7).

$$\begin{array}{ll} \text{Inertia} & \textcircled{1}\ lower\ bound: \tfrac{1}{2}\gamma^{-1}_{RoCoF}\Delta P_{Step} \\ & \textcircled{2}\ lower\ bound: \tfrac{1}{2}T_G\left(\text{term}_1 - \sqrt{\text{term}_2}\right) \\ & \textcircled{3}\ lower\ bound: \mathcal{R}^{-1}(D_{EQU})\gamma_{Nadir} \\ & \textcircled{4}\ upper\ bound: \tfrac{1}{2}T_G\left(\text{term}_1 + \sqrt{\text{term}_2}\right) \\ & \textcircled{5}\ upper\ bound: \tfrac{1}{2}(D_{EQU} + F_G)T_G \\ \text{Damping} & \textcircled{6}\ lower\ bound: \gamma^{-1}_{QSS}\Delta P_{Step} \end{array} \tag{8a}$$

IV. Case Studies and Analysis

A IEEE 30 bus test system with two wind farms is applied to demonstrate the effectiveness of the proposed criterion. Both multidimensional frequency parameters provided by conventional generators and converters is sorted out in table I.

TABLE I
MULTIDIMENSIONAL FREQUENCY PARAMETER CONFIGURATIONS

Type	H [p.u.]	D [p.u.]	R [p.u.]	F [p.u.]	T [s]
OCGT	6.0	0.6	0.05	0.35	8.0
Converter (Virtual Inertia)	6.0	0.6	-	-	-
Converter (Droop)	-	-	0.01	-	-

It can be found that the H-D support set in fig. 2 formed by (8a) is an approximate convex polyhedron. In the aforementioned former five bounds in (8a) concerning inertia parameters, 2 and 4 represent redundant constraints, whereas 1, 3, and 5 are active constraint that restrict the actual feasible area of the H-D support set. Remarkably, the RoCoF constraint termed as 1, nadir constraint termed as 3, and Qss constraint termed as 6 are commonly-used frequency dynamic requirements, these constraints in frequency-oriented studies are also the main types of constraints that play a role in the constructions of H-D support set, demonstrating the feasibility of H-D support set in this work.

The difference from previous studies lies in that this letter additionally identifies more bounding conditions, and these refined bounding conditions, along with the addition of RoCoF,

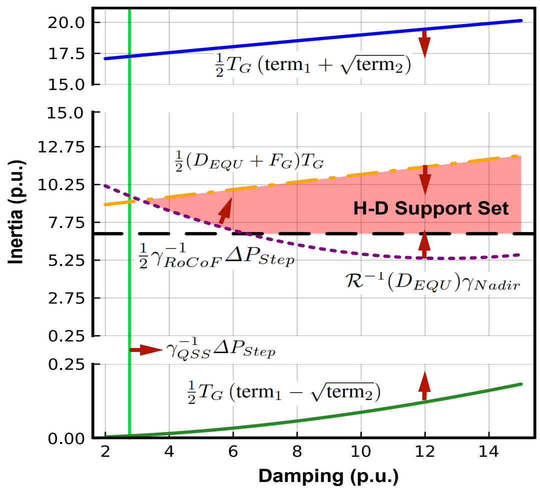

Fig. 2. The feasible area of the H-D support set in the low inertia system

nadir, and Qss constraints, form a relatively closed polyhedron region. In Fig. 2, the scale of the H-D set intuitively demonstrates the feasible range of multidimensional frequency parameters. By specifically increasing the upper bound of inertia H_{EQU}, termed as 5, the range of the H-D set can be further expanded. Nevertheless, the upper bound of H_{EQU} can be indirectly achieved by increasing the amount of equivalent damping parameter D_{EQU}.

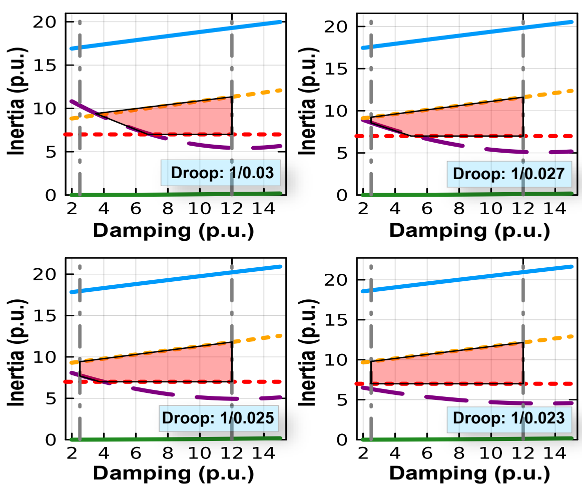

Fig. 3. The variation in the extent of the H-D support set across different frequency droop parameter configurations

Furthermore, the scope of the H-D support sets exhibits variation contingent upon droop parameter settings. However, once the droop parameter surpasses a threshold of $1/0.023$, the H-D set becomes invariant (see Fig. 3), and it is exclusively determined by the inertia bounds 1 and 3. Fig. 4 records the geometric characteristic of these H-D sets under different multidimensional frequency parameter configurations.

This observation highlights that for a public grid characterized by a comparatively low droop parameter (indicative of a relatively high frequency adjustment capability), further augmentation of system droop performance will not progressively expand the feasible operating region of the H-D set. Instead, it becomes imperative to enhance the frequency safety margin by increasing system inertia and damping. In conjunction

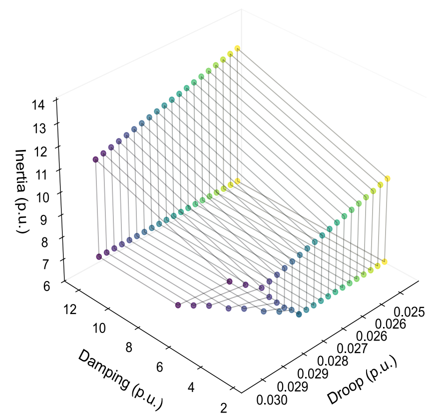

Fig. 4. The geometric structure defined by the ensemble of H-D sets across various multidimensional frequency parameter configurations

with the preceding analysis, H-D support set offers more precise and intuitive recommendations for frequency parameters tuning and system operation optimization.

V. Conclusion

This letter details an analytical solution of multidimensional frequency bounds and introduces a new criterion, termed the H-D support set, to characterize the feasible range of frequency parameters in low inertia grids. Furthermore, the polyhedral extent of H-D support set is comparatively assessed across various frequency parameter configurations. The proposed methodology facilitates a clear visualization and comparative evaluation of the impact of different frequency parameters on the operating interval of the system, thereby serving as a guideline for ensuring that the system remains within its inherent feasible range.

References

[1] S. A. Hosseini, M. Toulabi, A. S. Dobakhshari, A. Ashouri-Zadeh, and A. M. Ranjbar, "Delay compensation of demand response and adaptive disturbance rejection applied to power system frequency control," *IEEE Transactions on Power Systems*, vol. 35, no. 3, pp. 2037–2046, 2020.

[2] S. A. Hosseini, M. Fotuhi-Firuzabad, P. Dehghanian, and M. Lehtonen, "Coordinating demand response and wind turbine controls for alleviating the first and second frequency dips in wind-integrated power grids," *IEEE Transactions on Industrial Informatics*, vol. 20, no. 2, pp. 2223–2233, 2024.

[3] U. Markovic, V. Häberle, D. Shchetinin, G. Hug, D. Callaway, and E. Vrettos, "Optimal sizing and tuning of storage capacity for fast frequency control in low-inertia systems," in *2019 International Conference on Smart Energy Systems and Technologies (SEST)*. IEEE, 2019, pp. 1–6.

[4] Y. Yuan, Y. Zhang, J. Wang, Z. Liu, and Z. Chen, "Enhanced frequency-constrained unit commitment considering variable-droop frequency control from converter-based generator," *IEEE Transactions on Power Systems*, vol. 38, no. 2, pp. 1094–1110, 2023.

[5] Y. Liu, D. Xie, and H. Zhang, "Frequency-constrained unit commitment considering typhoon-induced wind farm cutoff and grid islanding events," *Journal of Modern Power Systems and Clean Energy*, vol. 12, no. 6, pp. 1760–1772, 2024.

[6] S. Cai, Y. Xie, Y. Zhang, W. Bao, Q. Wu, C. Chen, and J. Guo, "Frequency constrained proactive scheduling for secure microgrid formation in wind power penetrated distribution systems," *IEEE Transactions on Smart Grid*, vol. 16, no. 2, pp. 989–1002, 2025.

[7] Y. Wang and G. Strbac, "Regional frequency-constrained planning for the optimal sizing of power systems via enhanced input convex neural networks," *IEEE Transactions on Sustainable Energy*, pp. 1–14, 2025.

[8] J. Wang, J. Zhang, M. Yang, Y. Wang, and N. Zhang, "Nodal frequency-constrained energy storage planning via hybrid data-model driven methods," *iEnergy*, vol. 4, no. 1, pp. 43–53, 2025.